Title

Biomechanical changes to Descemet's membrane precede endothelial cell loss in an early-onset murine model of Fuchs endothelial corneal dystrophy

Authors

Leonard, Brian C
Jalilian, Iman
Raghunathan, Vijay Krishna
et al.

Publication Date

2019-03-01

DOI

10.1016/j.exer.2018.11.021

Peer reviewed

HHS Public Access

Author manuscript

Exp Eye Res. Author manuscript; available in PMC 2020 March 01.

Published in final edited form as:

Exp Eye Res. 2019 March ; 180: 18–22. doi:10.1016/j.exer.2018.11.021.

Biomechanical changes to Descemet's membrane precede endothelial cell loss in an early-onset murine model of Fuchs endothelial corneal dystrophy

Brian C. Leonard[#a], **Iman Jalilian**[#a], **Vijay Krishna Raghunathan**[b,c,d], **Wei Wang**[e], **Albert S. Jun**[e], **Christopher J. Murphy**[a,f], and **Sara M. Thomasy**[a,f,*]

[a]Department of Surgical and Radiological Sciences, School of Veterinary Medicine, University of California, Davis, Davis, California, United States

[b]The Ocular Surface Institute, University of Houston, Houston, Texas, United States

[c]Department of Basic Sciences, College of Optometry, University of Houston, Houston, Texas, United States

[d]Department of Biomedical Engineering, Cullen College of Engineering, University of Houston, Houston, Texas, United States

[e]Wilmer Eye Institute, Johns Hopkins Medical Institutions, Baltimore, Maryland, United States

[f]Department of Ophthalmology & Vision Sciences, School of Medicine, University of California, Davis, Davis, California, United States

[#] These authors contributed equally to this work.

Abstract

Early-onset Fuchs endothelial corneal dystrophy (FECD) has been associated with nonsynonymous mutations in collagen VIII α2 (COL8A2), a key extracellular matrix (ECM) protein in Descemet's membrane (DM). Two knock-in strains of mice have been generated to each express a mutant COL8A2 protein (*Col8a2*$^{L450W/L450W}$ and *Col8a2*$^{Q455K/Q455K}$) that recapitulate the clinical phenotype of early-onset FECD including endothelial cell loss, cellular polymegathism and pleomorphism, and guttae. Due to abnormalities in ECM protein composition and structure in FECD, the stiffness of DM in *Col8a2* knock-in mice and wildtype (WT) controls was measured using atomic force microscopy at 5 and 10 months of age, coinciding with the onset of FECD phenotypic abnormalities. At 5 months, only sporadic guttae were identified via *in vivo* confocal microscopy (IVCM) in *Col8a2*$^{Q455K/Q455K}$ mice, otherwise both strains of *Col8a2* transgenic mice were indistinguishable from WT controls in terms of endothelial cell density and size. By 10 months of age, *Col8a2*$^{L450W/L450W}$ and *Col8a2*$^{Q455K/Q455K}$ mice developed reduced corneal endothelial density, increased endothelial cell area and guttae, with the *Col8a2*$^{Q455K/Q455K}$ strain

[*]Corresponding author. Department of Surgical and Radiological Science, School of Veterinary Medicine, 1 Shields Avenue, University of California, Davis, CA 95616, USA, smthomasy@ucdavis.edu (S.M. Thomasy).

exhibiting a more severe phenotype. However, at 5 months of age, prior to the development endothelial cell abnormalities, *Col8a2*$^{L450W/L450W}$ and *Col8a2*$^{Q455K/Q455K}$ mice knock-in mice had reduced tissue stiffness of DM that was statistically significant in the *Col8a2*$^{Q455K/Q455K}$ mice when compared with wildtype controls. These data indicate that alterations in the tissue compliance of DM precede phenotypic changes in endothelial cell count and morphology and may play a role in onset and progression of FECD.

Keywords

Fuchs; cornea; endothelial; biomechanics; Descemet's membrane

Fuchs endothelial corneal dystrophy (FECD) is a primary, degenerative disorder of the corneal endothelium which leads to endothelial cell loss and corneal edema, progressing to vision impairment and blindness if left untreated (Vedana et al., 2016). In fact, patients with FECD represent the group with the highest indication for corneal transplantation (Eye Bank of America, 2017). This disease can be subcategorized based on the age at which FECD develops, early- or late-onset, with late-onset being much more common. Among the most common clinical signs are the presence of guttae, excrescences of abnormal extracellular matrix (ECM), and thickening of Descemet's membrane (DM) (Borboli and Colby, 2002; Krachmer et al., 1978). Descemet's membrane is the basement membrane complex which corneal endothelial cells secrete and reside upon, with a principle component being collagen VIII (COL8) (Levy et al., 1996). Over the past 20 years, multiple studies have associated genetic alterations with FECD, with mutations in the COL8 gene being identified in early-onset FECD patients (Biswas et al., 2001; Mok et al., 2009). Two of the nonsynonymous mutations in the COL8 α2 (COL8A2) subunit, L450W and Q455K, result in abnormal deposition of COL8A2 protein throughout DM (Gottsch et al., 2005).

Numerous studies document that the biophysical cues presented by the ECM are key determinants of cell phenotype and function (Vogel and Sheetz, 2006; Wells, 2008). Cells can perceive force exerted by ECM proteins/ligands, their position, and shape within the context of a tissue and alter signaling pathways to maintain homeostasis, a process termed mechanotransduction (Mammoto and Ingber, 2009; Panciera et al., 2017). However, in disease states such as chronic inflammation and fibrosis, the ECM composition can be altered, leading to changes in tissue elastic modulus. The change in elastic modulus activates mechanotransduction signaling pathways which, in turn, alter a wide array of fundamental cellular processes. Recent studies document composition, structural and biomechanical changes in DM from patients with FECD. Gene expression profiling of DM-endothelial complexes from FECD patients revealed marked upregulation of ECM genes: collagens (I, III, XVI), fibronectin, agrin, clusterin, transforming growth factor beta-induced (TGFBI), integrin α4, ZEB1 and Snail1 (Okumura et al., 2015; Weller et al., 2014). Additional studies documented alterations in the biophysical attributes of DM from FECD and guttae-affected patients (Thomasy et al., 2017; Xia et al., 2016). FECD patients had more widely-spaced collagen fibrils in DM, resulting in a reduced tissue elastic modulus and a softer DM (Xia et al., 2016). The biophysical attributes of DM have not been reported in mouse models with mutations in the *Col8a2* gene.

Despite the knowledge that ECM deposition in DM is a common feature of FECD, questions remain regarding the biophysical impact of altered ECM on corneal endothelial cells. To help answer some of these questions, we utilized two mouse models of early-onset FECD with knock-in mutations in the *Col8a2* gene which recapitulate the human condition including corneal endothelial cell loss, altered endothelial cell morphology, and guttae (Jun et al., 2012; Meng et al., 2013). This study sought to document biophysical attributes of DM in the mouse model of early-onset FECD and correlate findings with the onset of phenotypic and cellular changes of FECD. We hypothesized that the composition and structure of DM in *Col8a2* transgenic mice would result in alterations in the tissue stiffness of DM when compared with WT controls. Importantly, we identified softening of DM that preceded cellular and clinical features of FECD. This finding indicates that abnormal ECM deposition corresponds to softening of DM that may potentiate a deleterious change in corneal endothelial cells, leading to endothelial cell loss and polymegathism.

Col8a2 knock-in mice (both $Col8a2^{L450W/L450W}$ and $Col8a2^{Q455K/Q455K}$) were engineered and genotyped as previously described (Jun et al., 2012; Meng et al., 2013), and cohorts of both knock-in mice and wildtype littermates were euthanized at either 5 months [n=6 animals per group (3 females, 3 males)] or 10 months [n=5 WT (2 females, 3 males); n=5 $Col8a2^{Q455K/Q455K}$ (3 females, 2 males); n=4 $Col8a2^{L450W/L450W}$ (2 females, 2 males)]. Animal husbandry and euthanasia protocols were approved by the Institutional Animal Care and Use Committee of Johns Hopkins Medical Institutions and performed according to the Association for Research in Vision and Ophthalmology resolution on use of animals in research. Immediately after euthanasia, quantitative assessment of endothelial cell density and cell polygonal area were determined using a commercially available *in vivo* confocal microscope with included software on all animals previously listed (Nidek Confoscan 3, Fremont, CA, USA). Endothelial cell density was manually counted from a single representative image. The mean endothelial cell area was determined by dividing the polygonal area by the total number of cells in the field from a single representative image. Subsequent to imaging, both eyes were enucleated with the right eye designated for measuring elastic modulus of Descemet's membrane using atomic force microscopy (AFM) [n=4 eyes per group (2 females, 2 males)] and the left eye designated for histologic examination and periodic acid Schiff staining of the endothelium and DM. The right eye was wrapped in sterile gauze soaked in saline, transported overnight on ice and processed the following day for AFM. Briefly, the cornea was dissected from the remainder of the globe, incubated in 2.5 mM EDTA in HEPES buffer for 30 minutes, sonicated for five minutes to remove endothelial cells. Using a modification of the SCIRT method, the cornea was placed into an AFM dish coated with cured dielectric silicone (Sylgard 527, Dow Corning, Midland, MI) with DM oriented upwards, SCIRT placed on top of the tissue was immobilized using a ring of cyanoacrylate glue around the perimeter of the cornea, Dulbecco's phosphate buffered saline was added to cure the glue and keep the tissue hydrated (Morgan et al., 2014). This method was carefully followed to avoid any glue-related artifacts in sample preparation during AFM measurements. The SCIRT along with the adhesive Sylgard polymer ensured the tissue was immobilized sufficiently. Using silicon nitride cantilevers (PNP-TR-50, Nano World, Switzerland), modified with a borosilicate bead (5 μm nominal radius), 5 indentation force vs. indentation depth curves were obtained

at 2 μm/s for each sample from at least 5 random locations around the center of the cornea (Thomasy et al., 2014). Maximum indentation force was set at 1 nN; during analyses regions of linear elasticity was determined to be between 50-200 nm of indentation depth. Since DM of the mouse ranges in thickness from 1.1 to 4.3 μm with age (Jun et al., 2006), the AFM tissue stiffness measurement localizes only DM and there is no contribution from the substratum (i.e corneal stroma). The left eye was fixed in 10% formalin, paraffin embedded and cut into 5 μm sections. The sections were stained with periodic acid Schiff (PAS) stain to highlight DM and guttae. Data are presented as mean ± standard deviation and group wise comparisons were conducted by one-way ANOVA with post-hoc multiple comparison tests (if $P < 0.05$) when appropriate using Prism 7 (GraphPad Software, La Jolla, CA).

Confocal biomicroscopy findings were consistent with previously reported findings (Jun et al., 2012; Meng et al., 2013). At 5 months of age, few guttae were visible in the *Col8a2*$^{Q455K/Q455K}$ mice, while none were detected in the *Col8a2*$^{L450W/L450W}$ and wildtype control mice (Figure 1A). By 10 months, both transgenic strains (*Col8a2*$^{L450W/L450W}$ and *Col8a2*$^{Q455K/Q455K}$) had guttae, being noticeably more abundant in the *Col8a2*$^{Q455K/Q455K}$ mice (Figure 1A). The guttae identified with clinical imaging were also present on histologic analysis of the cornea as PAS positive excresences on DM and between corneal endothelial cells sporadically in *Col8a2*$^{L450W/L450W}$, yet more frequently in *Col8a2*$^{Q455K/Q455K}$ at 10 months of age, consistent with the IVCM findings (Figure 1B). There were no PAS positive guttae identified in the both *Col8a2* knock-in strains of mice at 5 months nor in WT at 5 or 10 months.

Using confocal biomicroscopy, corneal endothelial cell density and mean endothelial cell size were calculated. At 5 months of age, there were no statistical differences between endothelial cell densities between groups (mean ± SD; WT: 2232 ± 64 cells/mm^2, *Col8a2*$^{L450W/L450W}$: 2098 ± 90 cells/mm^2, *Col8a2*$^{Q455K/Q455K}$: 2202 ± 147 cells/mm^2; $P = 0.08$). By 10 months of age there was a significant reduction in corneal endothelial cell density in the *Col8a2*$^{Q455K/Q455K}$ knock-in mice when compared with wildtype controls (mean ± SD; WT: 2073 ± 116 cells/mm^2, *Col8a2*$^{Q455K/Q455K}$: 1404 ± 133 cells/mm^2; $P < 0.005$). *Col8a2*$^{L450W/L450W}$ mice had a reduced (mean ± SD; *Col8a2*$^{L450W/L450W}$: 1615 ± 199 cells/mm^2), but not significant, endothelial cell density compared to WT controls (Figure 2A). There were no significant differences detected in the mean size of corneal endothelial cells at 5 months of age between the groups (mean ± SD; WT: 448.3 ± 13.0 μm^2, *Col8a2*$^{L450W/L450W}$: 477.3 ± 19.6 μm^2, *Col8a2*$^{Q455K/Q455K}$: 455.8 ± 31.0 μm^2; $P > 0.05$) (Figure 2B). At 10 months of age, there was a significant increase in the endothelial cell size in *Col8a2*$^{Q455K/Q455K}$ mice when compared with wildtype controls (mean ± SD; WT: 483.4 ± 25.2 μm^2, *Col8a2*$^{Q455K/Q455K}$: 717.6 ± 65.5 μm^2; $P < 0.005$), and increased, but not significant, endothelial cell size between *Col8a2*$^{L450W/L450W}$ (*Col8a2*$^{L450W/L450W}$: 626.2 ± 74.7 μm^2) and WT controls (Figure 2B). There were no differences detected in tissue stiffness with respect to gender within and between any of the groups.

Since early-onset FECD patients have a large amount of disorganized COL8A2 which localizes to DM, we investigated the biophysical consequence of this change in ECM composition in *Col8a2* mutant knock-in mice (Gottsch et al., 2005). We performed AFM to measure tissue stiffness on decellularized DM from both *Col8a2* knock-in mutants and WT

controls. Interestingly, at the 5 month time point, there was already a significant reduction in tissue stiffness of DM from *Col8a2*$^{Q455K/Q455K}$ mice by 39% when compared to WT controls (mean ± SD; WT: 6.76 ± 2.68 kPa, *Col8a2*$^{Q455K/Q455K}$: 4.10 ± 2.17 kPa; $P < 0.0001$; Figure 2C). Also, there was a 10% reduction in DM stiffness in *Col8a2*$^{L450W/L450W}$ mice at 5 months of age when compared with controls (*Col8a2*$^{L450W/L450W}$: 6.08 ± 2.43 kPa) which was not statistically significant ($P = 0.6$). In both *Col8a2* knock-in strains the tissue stiffness of DM further reduced to 66% (L450W) and 57% (Q455K) of normal at the 10-month timepoint (mean ± SD; WT: 10.05 ± 7.34 kPa, *Col8a2*$^{L450W/L450W}$: 3.42 ± 2.02 kPa, *Col8a2*$^{Q455K/Q455K}$: 4.37 ± 3.92 kPa; $P < 0.0001$; Figure 2C). These data indicate that reduced tissue elastic modulus (decreased stiffness) preceded the alterations in corneal endothelial cell density and cell size.

The current study evaluated alterations in the biophysical properties of DM in an early-onset murine model of FECD at two different time points, 5 and 10 months of age. The clinical diagnostic imaging and histopathologic changes in the *Col8a2*$^{L450W/L450W}$ and *Col8a2*$^{Q455K/Q455K}$ mice were similar to previous studies, with the *Col8a2*$^{Q455K/Q455K}$ mice exhibiting a more severe phenotype (Jun et al., 2012; Meng et al., 2013). At 5 months of age, only rare guttae were visible in the *Col8a2*$^{Q455K/Q455K}$ mice on confocal biomicroscopy; however, by 10 months of age, both groups evidenced guttae, lower endothelial cell density and increased mean endothelial cell area. Importantly, a reduction in the stiffness of DM in *Col8a2* mice preceded the major phenotypic changes seen in corneal endothelial cells. The decreased stiffness became more exaggerated as the stiffness of DM in WT mice increased nearly two-fold by 10 months of age. These findings led us to conclude that (1) an increase in DM stiffness during maturation is a normal finding in mice and (2) *Col8a2* knock-in mice have an intrinsically lower DM stiffness when compared with WT controls, which may be necessary for normal endothelial cell maintenance and function and (3) changes in DM stiffness and composition may precede and contribute to onset and progression of the endothelial cell changes in early-onset FECD.

One of the hallmark features of FECD is the deposition of abnormal ECM throughout DM. Collagen VIII α1 and α2 proteins colocalize to the anterior banded layer of DM in stochiometric equivalents and relatively absent throughout the remainder of DM (Gottsch et al., 2005). However, FECD patients have both altered composition and organization of COL8A1 and COL8A2 throughout DM (Gottsch et al., 2005). In early-onset FECD, it has been suggested that this deposition of abnormal COL8A2 into the fetal anterior banded layer may be an initiating event that leads to endothelial dysfunction (Gottsch et al., 2005). In fact, the continued deposition of mutant COL8A2 protein into additional layers of DM in FECD after birth could be due to endothelial cell upregulation of COL8A1 and COL8A2 synthesis, in an attempt to normalize their basement membrane. Ultrastructural studies of early-onset FECD corneas have demonstrated the presence of a posterior layer of DM short strips and transverse bands, presumed to be wide-spaced collagen that contain collagen VIII (Gottsch et al., 2005; Levy et al., 1996). The resulting DM would have increased amounts of unstructured collagen, altering the biomechanics of DM, and result in endothelial cell dysfunction.

The role of mechanotransduction, a process by which a cell "senses" the extracellular cues and transforms them into biochemical signals, has become increasingly important in our understanding of cell behavior (Panciera et al., 2017). Cells can detect changes in ECM stiffness and topography, converting them into intracellular signals and ultimately, a cellular response (Ali et al., 2016). Transmembrane proteins interact with the actin cytoskeleton to transmit information to cytoplasmic and nuclear targets which affect protein interactions and gene transcription regulating cell proliferation, survival, polarity and many others (Maniotis et al., 1997; Schwarz and Gardel, 2012). Interestingly, tissue fibrosis is seen as a sequela to chronic inflammatory conditions, and *in vitro*, as well as *in vivo* studies have demonstrated that the excessive ECM deposition associated with chronic inflammation leads to increased tissue stiffness (Jorgenson et al., 2017; Nowell et al., 2016). Fibrosis is the result of excessive ECM (including collagens) deposition following which the fibrils are tightly organized by contractile elements, causing the ECM to adopt a stiffer composition which directly affects neighboring cell behavior (Ehrlich and Hunt, 2012; Wells, 2013). In the context of FECD, there is increased collagen deposition yet the ECM is softer when compared to normal and is likely due to abnormal arrangement and spacing of the collagen fibrils (Xia et al., 2016). The observation of reduced stiffness of ECM in *Col8a2* transgenic mice and FECD, rather than increased stiffness as seen in other pathologies associated with excessive ECM deposition, appears to mimic the mechanobiology seen in FECD. Additional studies are underway to evaluate the role of decreased ECM stiffness on signaling pathways in corneal endothelial cells and how it affects proliferation and differentiation, cell size, Na/K-ATPase activity and maintenance of corneal deturgescence.

Overall the data demonstrate alterations in the stiffness of DM prior to phenotypic changes in corneal endothelial cells and endothelial cell loss. We speculate that the L450W and Q455K *Col8a2* mutations result in improper protein structure, preventing the tight packaging of COL8A1 and COL8A2 in the fetal anterior banded layer, resulting in a softer DM. As DM matures and thickens with the deposition of other basement collagens forming the posterior nonbanded layer, DM likely stiffens over time. We further speculate that the softer DM is "sensed" by the endothelial cells via mechanotransduction and these endothelial cells continue to synthesize/deposit abnormal COL8A2 that is widely-spaced and unstructured. Therefore, as the normal animal matures a more tightly packed and orderly arranged DM will stiffen, while the DM of *Col8a2* transgenic mice will remain soft. Further studies are required to determine the impact of these biophysical changes in the ECM on corneal endothelial cells.

Acknowledgments

FUNDING STATEMENT:

This work was supported by the by the National Institutes of Health K08EY028199 (BCL), K08EY021142 (SMT), R01EY016134 (CJM), the NEI core grant P30EY12576, start-up funds from the School of Veterinary Medicine, University of California, Davis (SMT) and partial funding through start-up fund from the University of Houston College of Optometry, Houston (VKR).

REFERENCES:

Ali M, Raghunathan V, Li JY, Murphy CJ, Thomasy SM, 2016 Biomechanical relationships between the corneal endothelium and Descemet's membrane. Exp Eye Res 152, 57–70. [PubMed: 27639516]

Eye Bank of America, 2017 2016 Eye Banking Statistical Report, pp. 1–99.

Biswas S, Munier FL, Yardley J, Hart-Holden N, Perveen R, Cousin P, Sutphin JE, Noble B, Batterbury M, Kielty C, Hackett A, Bonshek R, Ridgway A, McLeod D, Sheffield VC, Stone EM, Schorderet DF, Black GC, 2001 Missense mutations in COL8A2, the gene encoding the alpha2 chain of type VIII collagen, cause two forms of corneal endothelial dystrophy. Hum Mol Genet 10, 2415–2423. [PubMed: 11689488]

Borboli S, Colby K, 2002 Mechanisms of disease: Fuchs' endothelial dystrophy. Ophthalmol Clin North Am 15, 17–25. [PubMed: 12064077]

Ehrlich HP, Hunt TK, 2012 Collagen Organization Critical Role in Wound Contraction. Adv Wound Care (New Rochelle) 1, 3–9. [PubMed: 24527271]

Gottsch JD, Zhang C, Sundin OH, Bell WR, Stark WJ, Green WR, 2005 Fuchs corneal dystrophy: aberrant collagen distribution in an L450W mutant of the COL8A2 gene. Invest Ophthalmol Vis Sci 46, 4504–4511. [PubMed: 16303941]

Jorgenson AJ, Choi KM, Sicard D, Smith KM, Hiemer SE, Varelas X, Tschumperlin DJ, 2017 TAZ activation drives fibroblast spheroid growth, expression of profibrotic paracrine signals, and context-dependent ECM gene expression. Am J Physiol Cell Physiol 312, C277–C285. [PubMed: 27881410]

Jun AS, Chakravarti S, Edelhauser HF, Kimos M, 2006 Aging changes of mouse corneal endothelium and Descemet's membrane. Exp Eye Res 83, 890–896. [PubMed: 16777092]

Jun AS, Meng H, Ramanan N, Matthaei M, Chakravarti S, Bonshek R, Black GC, Grebe R, Kimos M, 2012 An alpha 2 collagen VIII transgenic knock-in mouse model of Fuchs endothelial corneal dystrophy shows early endothelial cell unfolded protein response and apoptosis. Hum Mol Genet 21, 384–393. [PubMed: 22002996]

Krachmer JH, Purcell JJ, Jr., Young CW, Bucher KD, 1978 Corneal endothelial dystrophy. A study of 64 families. Arch Ophthalmol 96, 2036–2039. [PubMed: 309758]

Levy SG, Moss J, Sawada H, Dopping-Hepenstal PJ, McCartney AC, 1996 The composition of wide-spaced collagen in normal and diseased Descemet's membrane. Curr Eye Res 15, 45–52. [PubMed: 8631203]

Mammoto A, Ingber DE, 2009 Cytoskeletal control of growth and cell fate switching. Curr Opin Cell Biol 21, 864–870. [PubMed: 19740640]

Maniotis AJ, Chen CS, Ingber DE, 1997 Demonstration of mechanical connections between integrins, cytoskeletal filaments, and nucleoplasm that stabilize nuclear structure. Proc Natl Acad Sci U S A 94, 849–854. [PubMed: 9023345]

Meng H, Matthaei M, Ramanan N, Grebe R, Chakravarti S, Speck CL, Kimos M, Vij N, Eberhart CG, Jun AS, 2013 L450W and Q455K Col8a2 knock-in mouse models of Fuchs endothelial corneal dystrophy show distinct phenotypes and evidence for altered autophagy. Invest Ophthalmol Vis Sci 54, 1887–1897. [PubMed: 23422828]

Mok JW, Kim HS, Joo CK, 2009 Q455V mutation in COL8A2 is associated with Fuchs' corneal dystrophy in Korean patients. Eye (Lond) 23, 895–903. [PubMed: 18464802]

Morgan JT, Raghunathan VK, Thomasy SM, Murphy CJ, Russell P, 2014 Robust and artifact-free mounting of tissue samples for atomic force microscopy. Biotechniques 56, 40–42. [PubMed: 24447138]

Nowell CS, Odermatt PD, Azzolin L, Hohnel S, Wagner EF, Fantner GE, Lutolf MP, Barrandon Y, Piccolo S, Radtke F, 2016 Chronic inflammation imposes aberrant cell fate in regenerating epithelia through mechanotransduction. Nat Cell Biol 18, 168–180. [PubMed: 26689676]

Okumura N, Minamiyama R, Ho LT, Kay EP, Kawasaki S, Tourtas T, Schlotzer-Schrehardt U, Kruse FE, Young RD, Quantock AJ, Kinoshita S, Koizumi N, 2015 Involvement of ZEB1 and Snail1 in excessive production of extracellular matrix in Fuchs endothelial corneal dystrophy. Lab Invest 95, 1291–1304. [PubMed: 26302187]

Panciera T, Azzolin L, Cordenonsi M, Piccolo S, 2017 Mechanobiology of YAP and TAZ in physiology and disease. Nat Rev Mol Cell Biol 18, 758–770. [PubMed: 28951564]

Schwarz US, Gardel ML, 2012 United we stand: integrating the actin cytoskeleton and cell-matrix adhesions in cellular mechanotransduction. J Cell Sci 125, 3051–3060. [PubMed: 22797913]

Thomasy SM, Raghunathan VK, Ali M, Jalilian I, Murphy CJ, 2017 Biomechanics of an *in vitro* model of Descemet's membrane in health and disease [abstract]. In: ARVO 2017 Annual Meeting Abstracts May 7-11; Baltimore, MD. .

Thomasy SM, Raghunathan VK, Winkler M, Reilly CM, Sadeli AR, Russell P, Jester JV, Murphy CJ, 2014 Elastic modulus and collagen organization of the rabbit cornea: epithelium to endothelium. Acta Biomater 10, 785–791. [PubMed: 24084333]

Vedana G, Villarreal G, Jr., Jun AS, 2016 Fuchs endothelial corneal dystrophy: current perspectives. Clin Ophthalmol 10, 321–330. [PubMed: 26937169]

Vogel V, Sheetz M, 2006 Local force and geometry sensing regulate cell functions. Nat Rev Mol Cell Biol 7, 265–275. [PubMed: 16607289]

Weller JM, Zenkel M, Schlotzer-Schrehardt U, Bachmann BO, Tourtas T, Kruse FE, 2014 Extracellular matrix alterations in late-onset Fuchs' corneal dystrophy. Invest Ophthalmol Vis Sci 55, 3700–3708. [PubMed: 24833739]

Wells RG, 2008 The role of matrix stiffness in regulating cell behavior. Hepatology 47, 1394–1400. [PubMed: 18307210]

Wells RG, 2013 Tissue mechanics and fibrosis. Biochim Biophys Acta 1832, 884–890. [PubMed: 23434892]

Xia D, Zhang S, Nielsen E, Ivarsen AR, Liang C, Li Q, Thomsen K, Hjortdal JO, Dong M, 2016 The Ultrastructures and Mechanical Properties of the Descement's Membrane in Fuchs Endothelial Corneal Dystrophy. Sci Rep 6, 23096. [PubMed: 26980551]

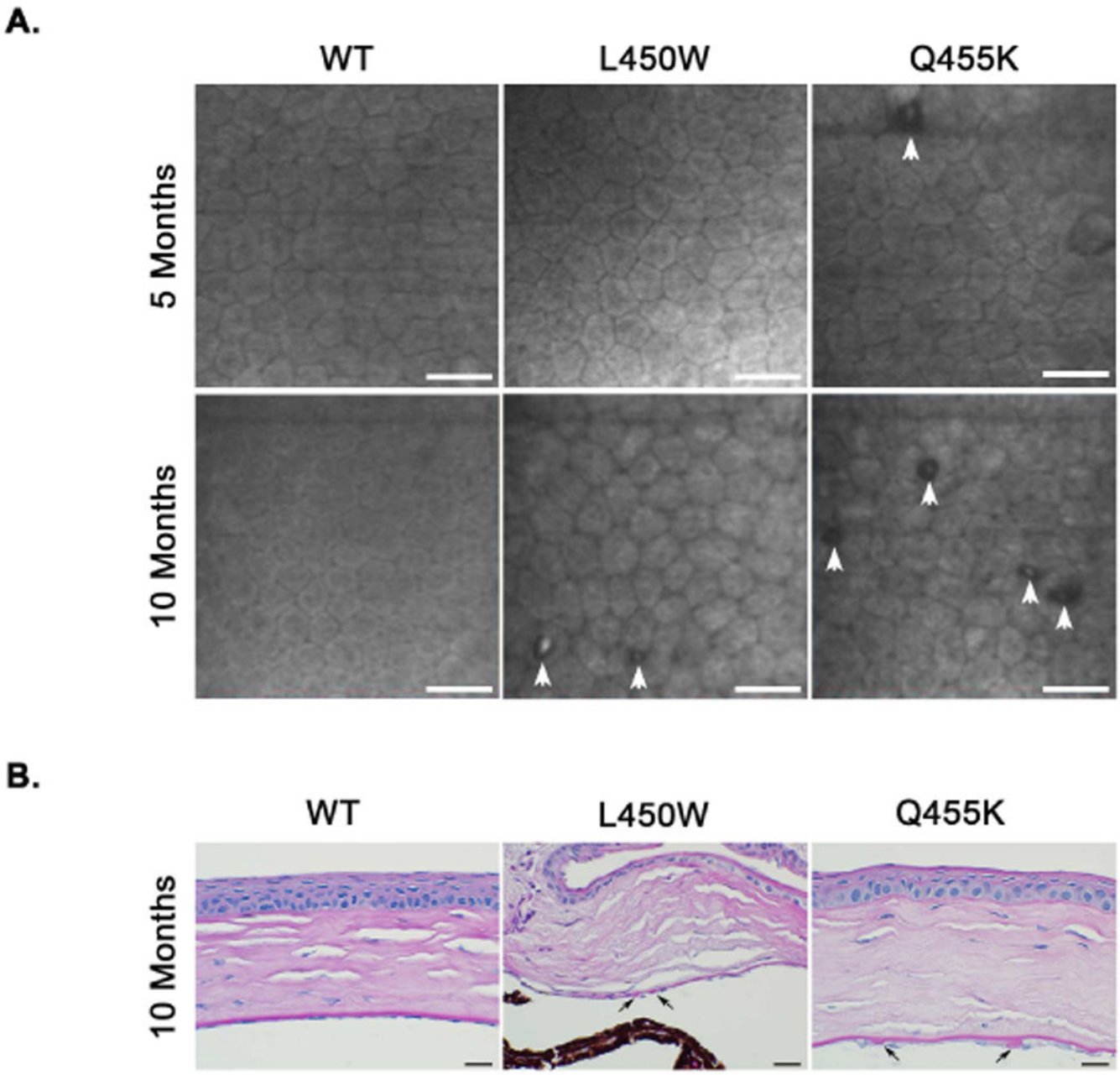

Figure 1. *Col8a2* mutant (L450W and Q455K) mice develop guttae (arrows) by 10 months of age.
(A) Confocal microscopy of enucleated globes via Confoscan 3 demonstrate few guttae (white arrows) in Q455K *Col8a2* mutants at 5 months, and more frequent at 10 months of age in both the L450W and Q455K *Col8a2* mutants. Scale bar equal to 50 μm. **(B)** Mice with L450W and Q455K mutations in *Col8a2* develop guttae (black arrows) by 10 months of age. Formalin fixed, paraffin embedded globes were sectioned at 5μm thickness and stained with periodic acid Schiff (PAS) to highlight Descemet's membrane and guttae. Scale bar equal to 20 μm. Representative images of animals in each group.

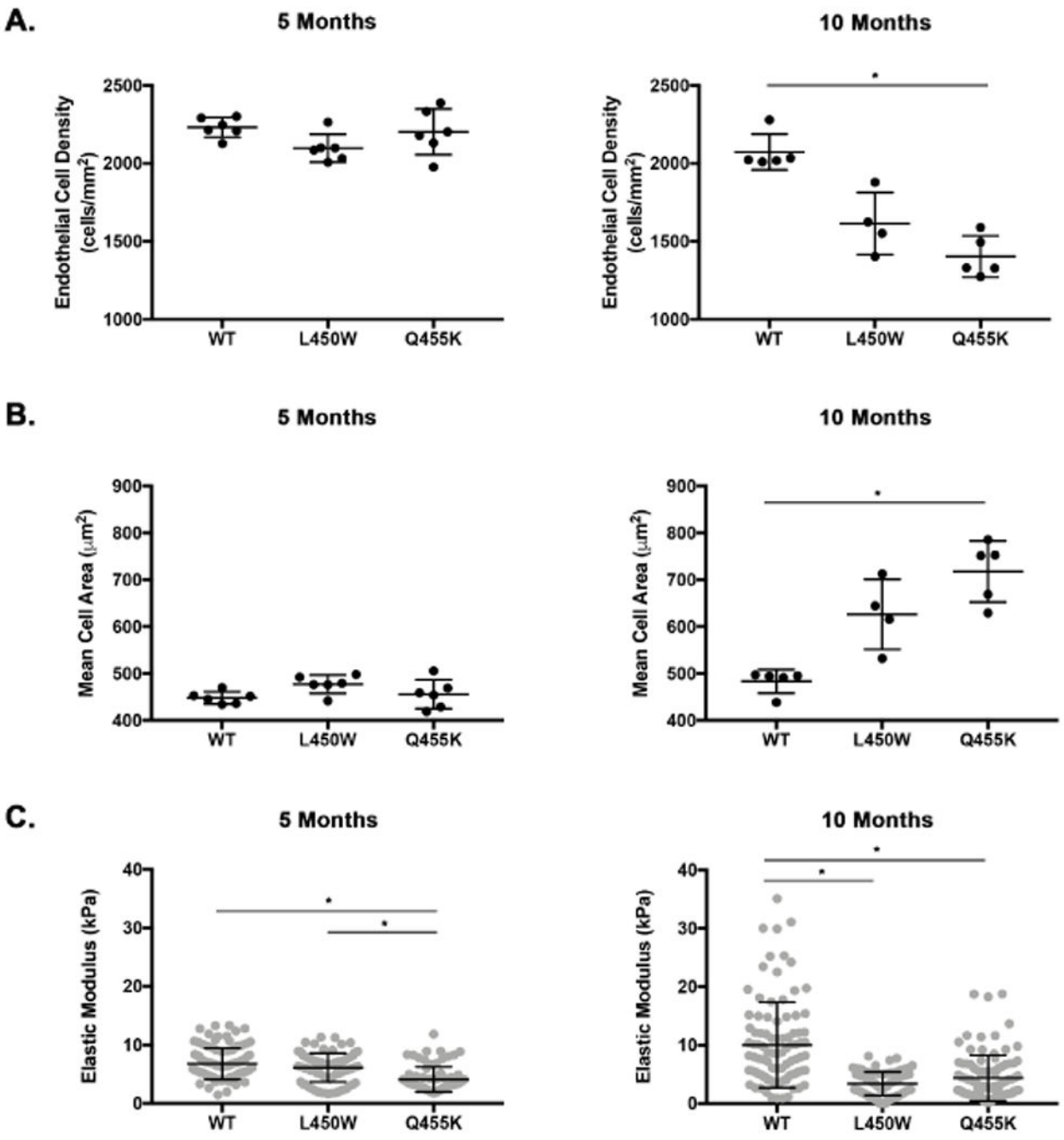

Figure 2. Reduction in tissue elastic modulus of DM in *Col8a2* knock-in mutant mice precedes endothelial cell loss and polymegathism.

(A) Corneal endothelial density determined by confocal microscopy, each dot represents endothelial cell count on one eye from each animal, analyzed from a single representative image. **(B)** Mean cell area determined via confocal microscopy, by dividing polygonal area by total number of cells in field. Each dot represents the calculated mean cell area from each animal within each group, analyzed from a single representative image. **(C)** Data represents the summation of AFM measurements of DM from all animals in each group combined (n=4

per group), with each dot representing a single AFM measurement (~80-100 measurements per group). Horizontal lines indicate mean and error bars represent SD. Kruskal-Wallis (nonparametric one-way ANOVA) with multiple comparisons post-hoc Dunn's test, * signifies $P < 0.05$.